A comparison of CPT-V_S correlations using a liquefaction case history database from the 2010-2011 Canterbury Earthquake Sequence

Clinton M Wood
Dept. of Civil Engineering – University of Arkansas, Fayetteville, AR, USA
Christopher R McGann
Dept. of Civil & Natural Resources Engineering – University of Canterbury, Christchurch, New Zealand
Brady R Cox
Dept. of Civil, Architectural, & Environmental Engineering – University of Texas at Austin, Austin, TX, USA
Russell Green
Dept. of Civil & Environmental Engineering – Virginia Tech, Blacksburg, VA, USA
Liam Wotherspoon
Dept. of Civil & Environmental Engineering – The University of Auckland, Auckland, New Zealand
Brendon A Bradley, Misko Cubrinovski
Dept. of Civil & Natural Resources Engineering – University of Canterbury, Christchurch, New Zealand

ABSTRACT

This study uses 44 high quality liquefaction case histories taken from 22 locations affected by the 2010-2011 Canterbury earthquake sequence to evaluate four commonly used CPT-V_S correlations (i.e., Robertson, 2009; Hegazy and Mayne, 2006; Andrus et al., 2007; McGann et al., 2015b). Co-located CPT soundings and V_S profiles, developed from surface wave testing, were obtained at 22 locations and case histories were developed for the M_w 7.1, 4 September 2010 Darfield and M_w 6.2, 22 February 2011 Christchurch earthquakes. The CPT soundings are used to generate V_S profiles using each of four CPT-V_S correlations. These correlated V_S profiles are used to estimate the factor of safety against liquefaction using the Kayen et al. (2013) V_S-based simplified liquefaction evaluation procedure. An error index is used to quantify the predictive capabilities of these correlations in relation to the observations of liquefaction (or the lack thereof). Additionally, the error indices from the CPT-correlated V_S profiles are compared to those obtained using: (1) the Kayen et al. (2013) procedure with surface wave-derived V_S profiles, and (2) the Idriss and Boulanger (2008) CPT-based liquefaction evaluation procedure. Based on the error indices, the evaluation procedures based on direct measurements of either CPT or V_S provided more accurate liquefaction triggering estimates than those obtained from any of the CPT-V_S correlations. However, the performance of the CPT-V_S correlations varied, with the Robertson (2009) and Hegazy and Mayne (2006) correlations performing relatively poorly for the Christchurch soils and the Andrus et al. (2007) and McGann et al. (2015b) correlations performing better. The McGann et al. (2015b) correlation had the lowest error indices of the CPT-V_S correlations tested, however, none of the CPT-V_S correlations provided accurate enough V_S predictions to be used for the evaluation of liquefaction triggering using the V_S-based liquefaction evaluation procedures.

1 INTRODUCTION

Shear wave velocity (V_S) is a fundamental parameter for all engineering materials and has become a desired, and in many cases vital, parameter for analyses in geotechnical earthquake engineering, including liquefaction triggering evaluation and site response. Although the direct measurement of V_S has become more commonplace today via methods such as surface wave testing, crosshole testing, downhole testing and/or seismic CPT (SCPT), routine geotechnical tests such as the cone penetration test (CPT) and standard penetration test (SPT) remain far more common for geotechnical site characterization. It is therefore useful to develop and use correlations to retrieve V_S information from these more common tests, and a number of correlations have been developed that relate CPT parameters such as cone tip resistance (q_c) and sleeve friction (f_s) to V_S. The benefits of such correlations include a potentially finer resolution of the V_S information with depth and an increased number of available V_S profiles due to the greater availability of CPT tests relative to surface wave or downhole/crosshole tests. CPT-V_S correlations are, however, not without limitations,

including poor performance in gravelly soils and potential errors/bias due to fundamental differences in the soil properties that influence the measured parameters of each test. This latter limitation is particularly important in regards to how soil properties affect small strain V_S measurements and large strain CPT measurements. For example, V_S measurements are heavily influenced by cementation and aging compared to the relatively minor influence these parameters have on CPT data (El-Sekelly et al., 2016). Previous comparisons of CPT-V_S correlations by McGann et al. (2015a,c) indicate these factors may be prevalent in Christchurch, as significant differences were observed for different CPT-V_S correlations and different soil types in the region.

In this paper, a liquefaction case history database with co-located CPT and V_S measurements at 22 sites throughout Christchurch is used to evaluate the performance of four CPT-V_S correlations in terms of the accuracy of the V_S profiles and their ability to correctly predict liquefaction triggering (or the lack thereof) for 44 case histories using the Kayen et al. (2013) (KEA13) liquefaction evaluation procedure. The performance of the correlations is compared to the performance of the KEA13

V_S-based and Idriss and Boulanger (2008) (I&B08) CPT-based liquefaction evaluation procedures using direct measurements (surface wave V_S and q_c). An error index is used to quantify the overall performance of each method and potential reasons for good or poor performance of the correlations are discussed.

2   2010-2011 CES LIQUEFACTION CASE HISTORIES

The 2010-2011 Canterbury Earthquake Sequence (CES) was comprised of up to 10 strong events that triggered liquefaction in the Canterbury region surrounding Christchurch, New Zealand (Quigley et al., 2013). These events were recorded by a dense network of strong motion stations and observations of liquefaction were well-documented across the region. The sites discussed herein were chosen based on their close proximity to strong motions stations and the availability of high-quality CPT soundings in the vicinity. Seismic surface wave testing was also performed at each site following the most devastating event in the CES, the M_w 6.2 Christchurch earthquake.

The CPT and V_S liquefaction case histories collected from this work are detailed in Green et al. (2014) and Wood et al. (2017), respectively. Average values of corrected V_S (V_{S1}), or corrected q_c (q_{c1Ncs}), and cyclic stress ratio (CSR) were calculated for the chosen critical layers at each site for both the M_w 7.1 Darfield and M_w 6.2 Christchurch earthquakes. Critical layers were developed on the guiding principle that the depth-thickness-density combination of the critical layer for a given site should be consistent with the observed liquefaction response of the site (Green et al., 2014; Green and Olson, 2015). For sites where no surficial evidence of liquefaction was observed, the critical layer was taken as the layer most susceptible to liquefaction based on the CPT data. Due to ambiguity in the selection of the critical layer at some sites, alternative critical layers were also defined.

To evaluate the efficacy of each simplified liquefaction evaluation procedure using the case history database, an error index approach was utilized. The Robertson and Wride (1998), Moss et al. (2006), and I&B08 CPT-based procedures were compared in Green et al. (2014), and it was shown that the I&B08 procedure produced the lowest error index and therefore performed best for this dataset. The Andrus and Stokoe (2000) and KEA13 V_S-based procedures were evaluated in Wood et al. (2017) using the surface wave-derived V_S profiles, and it was determined that the KEA13 procedure provided the lowest error index and therefore performed best for this dataset.

3   DEVELOPMENT OF SHEAR WAVE VELOCITY PROFILES

Five separate V_S profiles are developed for each case history site via direct measurement of V_S using surface wave methods (referred to as SW-V_S) and via correlations from CPT soundings using one of the four CPT-V_S correlations available in the literature (referred to as CPT-V_S). Surface wave testing was conducted as close as practically possible to the CPT location to ensure similar material was measured using each method. However, it should be noted that surface wave methods sample much

larger volumes of soil due to the necessity of using long sensor arrays on the surface compared to the relatively small volume of soil sampled with the CPT.

3.1   Shear Wave Velocity Profiles from Surface Wave Methods

Surface wave testing was conducted at each case history site to resolve the shear stiffness and layering. A combination of active source [Spectral Analysis of Surface Waves (SASW), Multi-channel Analysis of Surface Waves (MASW)] and passive source [1D and 2D Micro-tremor array measurements (MAM)] were used. For the active testing, a linear array of 24, 4.5 Hz geophones was used with an equal spacing (dx) between geophones of either 0.9 m or 1.5 m (total array length of either 20.7 m or 34.5 m, respectively). The same linear array was used for 1D passive testing and where possible an L-shaped array with geophone spacing of 1.5 m was utilized for 2D MAM.

For SASW, a single source located one receiver spacing off the end of the array was utilized. Individual receiver pairs were chosen from the array of 24 receivers to maintain a source-to-first-receiver distance equal to the first-to-second-receiver distance. For MASW, multiple source offsets were used with source locations of 4.6 m, 9.1 m, and 18.3 m from the first receiver. Five blows from a 4.5 kg sledgehammer were stacked at each source location. For 1D and 2D MAM, a total of 10, 32-second long records were recorded for each array setup.

The surface wave data was analyzed to develop individual experimental dispersion curves for each method. The SASW data was analyzed using the phase unwrapping method to develop dispersion curves for each receiver spacing. The MASW data was analyzed using the frequency domain beamformer method (Zywicki, 1999) for each source offset. The 1D MAM data was analyzed using the slowness-frequency (p-f) transformation, and the 2D MAM was analyzed using the 2D frequency domain beamformer method.

Once individual dispersion curves were developed, a mixed-method composite dispersion curve was generated based on all of the experimental dispersion curves. The dispersion data were divided into 30 wavelength bins equally-spaced in terms of a log distribution. The mean phase velocity and associated standard deviation was then calculated for each bin, resulting in an experimental dispersion curve with associated uncertainty. The V_S profile for each site was then generated by solving the inverse problem in WinSASW (Joh, 1996). Because of the inherent non-uniqueness involved in solving the inverse problem, the CPT soundings were used to inform the choice of layers (thickness and depth) during the inversion process. While this a-priori information from the CPT can provide valuable information to constrain the layering at the site, perfect agreement between the CPT layering and the V_S layering should not be expected. The soil properties which influence the cone tip resistance (q_c) and sleeve friction (f_s) differ from those that influence the small strain V_S (e.g., q_c is sensitive to density changes, V_S is more influenced by microstructure). Of particular importance for Christchurch is the influence of interbedded sands and gravels or gravelly sands on q_c readings (i.e., gravel that impacts the

cone tip typically causes unrealistically high tip resistances). While these soil conditions can significantly influence the q_c values, the influence on V_S is far more subdued as the global stiffness of the material is governed by the soil matrix.

To solve the inverse problem (i.e., theoretical fit to the experimental dispersion curve) a top-down forward modeling approach was utilized where the model was initially a one-layer half-space and only the short wavelength data was fit. Additional layers were added to the profile as required to fit the experimental dispersion data or as shown to exist by the CPT results. During this process, the dispersion curve was fit by-eye. At each stage in the process, velocity and thickness alternatives were considered to ensure the most appropriate solution was achieved. After reaching an acceptable by-eye solution, the automated least-squares inversion in WinSASW was used to ensure the best fit was achieved. A complete discussion of the surface wave testing and analysis is provided in Wood et al. (2017).

3.2   Shear wave Velocity Profiles from CPT-V_S Correlations

Four CPT-V_S correlation are examined in this study. Three are representative of the most commonly-used general soil CPT-V_S correlations developed from global datasets (Andrus et al., 2007; Hegazy and Mayne, 2006; Robertson, 2009). The fourth correlation (McGann et al., 2015b), was developed using Christchurch soils and has previously shown favorable comparisons with SW-V_S profiles obtained at Christchurch strong motion stations (McGann et al., 2015c). The following sections provide a brief discussion of each CPT-V_S correlation along with the equations used to obtain V_S profiles for each case history site.

3.2.1   Andrus et al. (2007) CPT-V_S Correlation

Andrus et al. (2007) (AEA07) present CPT-V_S correlations for general soils of Holocene, Pleistocene, and Tertiary ages. The surficial soils in Christchurch are of Holocene age, thus the Holocene-only correlation was selected:

$$V_S = 2.27q_t^{0.412}\,I_c^{0.989}\,z^{0.033} \qquad [1]$$

where q_t is the pore pressure-corrected cone tip resistance in kPa, I_c is the soil behavior type index (Robertson and Wride, 1998), z is the depth in meters, and V_S is in m/s.

3.2.2   Hegazy and Mayne (2006) CPT-V_S Correlation

The correlation of Hegazy and Mayne (2006) (H&M06):

$$V_S = 0.0831q_{c1N}\exp(1.7861+I_c)\,(\sigma'_{v0}/p_a)^{0.25} \qquad [2]$$

was developed based on 31 clay soil sites and 42 general soil sites located in the United States, Japan, and Europe. In Equation 2, q_{c1N} is the normalized tip resistance, σ'_{v0} is the vertical effective stress, p_a is the atmospheric pressure, and V_S is in m/s..

3.2.3   Robertson (2009) CPT-V_S Correlation

The CPT-V_S correlation of Robertson (2009) was developed from a global dataset of primarily general soil sites with Holocene and Pleistocene-age soils. The correlation (Rob09) is given as:

$$V_S = [10^{0.55\,I_c+1.68}((q_t - \sigma_{v0})/p_a)]^{0.5} \qquad [3]$$

where σ_{v0} is the vertical total stress, q_t, σ_{v0}, and p_a are all expressed in the same units, and V_S is in m/s.

3.2.4   McGann et al. (2015b) CPT-V_S Correlation

The Christchurch-specific CPT-V_S correlation of McGann et al. (2015b) was developed from 86 SCPTu sites located throughout the general Christchurch, New Zealand area. This correlation (MEA15) is given as:

$$V_S = 18.4q_t^{0.144}\,f_s^{0.0832}\,z^{0.278} \qquad [4]$$

where f_s is the cone frictional resistance. In this equation, q_t and f_s are expressed in units of kPa, z is expressed in meters, and V_S is in units of m/s. All of the SCPTu used to develop this correlation were performed after the 2010 Darfield event, and about 30 were performed after the February 2011 event. As discussed in McGann et al. (2015a), evidence indicates that any aging effects present in the soil were destroyed by the earthquakes and that the correlation is based on the new, de-aged, soil fabric.

4   EVALUATION OF CPT-V_S CORRELATIONS

The correlations are assessed by direct comparison of estimated V_S profiles (CPT-V_S) to surface wave derived V_S profiles (SW-V_S) and by comparing the performance of each correlation at assessing liquefaction response using the case history database. Although for many of the comparisons the SW-V_S values are used as the baseline measurement, this does not mean these values are 100% accurate. These values simply provide a comparison baseline for the analysis and discussion of the data.

4.1   Comparison of SW-V_S and CPT-V_S Profiles

Figure 1 shows a comparison between the SW-V_S profile and the CPT-V_S profiles for each of the four considered correlations at one of the case study sites. Approximate layer boundaries are indicated by major changes in the CPT profile, and the differences between the SW-V_S and CPT-V_S values are natural consequences of the different discretization in each method. Figure 1 also emphasizes the variation in the CPT-V_S returned by each correlation. The 100-200 m/s range in the measured/predicted V_S at this site is not representative of all of the case study sites, but there is variation to some degree at all sites.

The bias between the SW-V_S and CPT-V_S is computed for all of the sites and shown in Figure 2. The V_S bias is computed as the ratio of the SW-V_S in each layer to
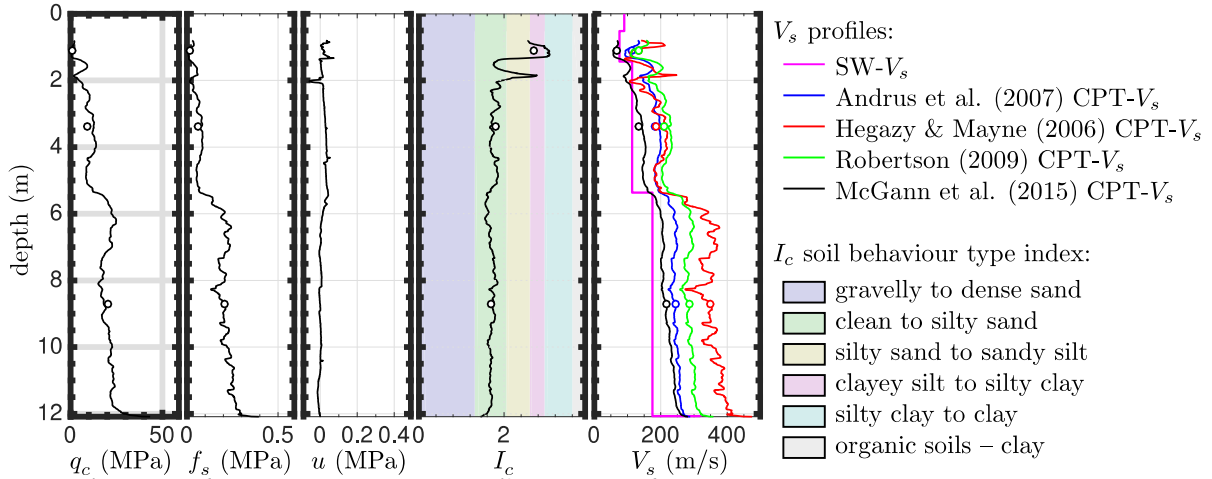
Figure 1. Comparison of SW-V$_S$ and CPT-V$_S$ profiles for a single site. CPT data and I$_c$ profile provided for reference.

the geometric mean of the CPT-V$_S$ values from a given correlation in that layer. The depth assigned to each bias data point is the center point of each respective SW-V$_S$ layer. The variation in this computed bias is shown in Figure 2 with the layer center depth, and with the geometric means of the cone tip resistance, frictional resistance, and soil behavior type index in each layer for all four correlations and all sites.

Comparing the results, the H&M06 and Rob09 CPT-V$_S$ correlations tend to systematically over-predict relative to the SW-V$_S$ (bias < 1), while the AEA07 and MEA15 correlations tend to be more balanced, with areas of over- and under-prediction. All of the correlations tend toward over-prediction with increasing depth and q$_c$, which may be a result of high q$_c$ values resulting from encountering gravel layers at deeper depths at many of the sites. The greatest

variation between the correlations is observed at the shallowest depths, lowest tip resistances, and highest I$_c$ values. Potential errors near the surface may be caused by the more horizontal travel path taken by shear waves when testing at near surface depths using the SCPT method, which was used to develop these correlations. It is also worth noting that the depth ranges covered by the SW-V$_S$ are often beyond the applicable ranges of the correlations, particularly at the shallowest depths, and it is likely that the correlations are being extrapolated in these areas. For example, Andrus et al. (2007) only considered SCPT measurements at depths > 3m in the development of AEA07 correlation, and the majority of sites used in the MEA15 correlation did not have SCPT-V$_S$ measurements at depths less than 2 m.
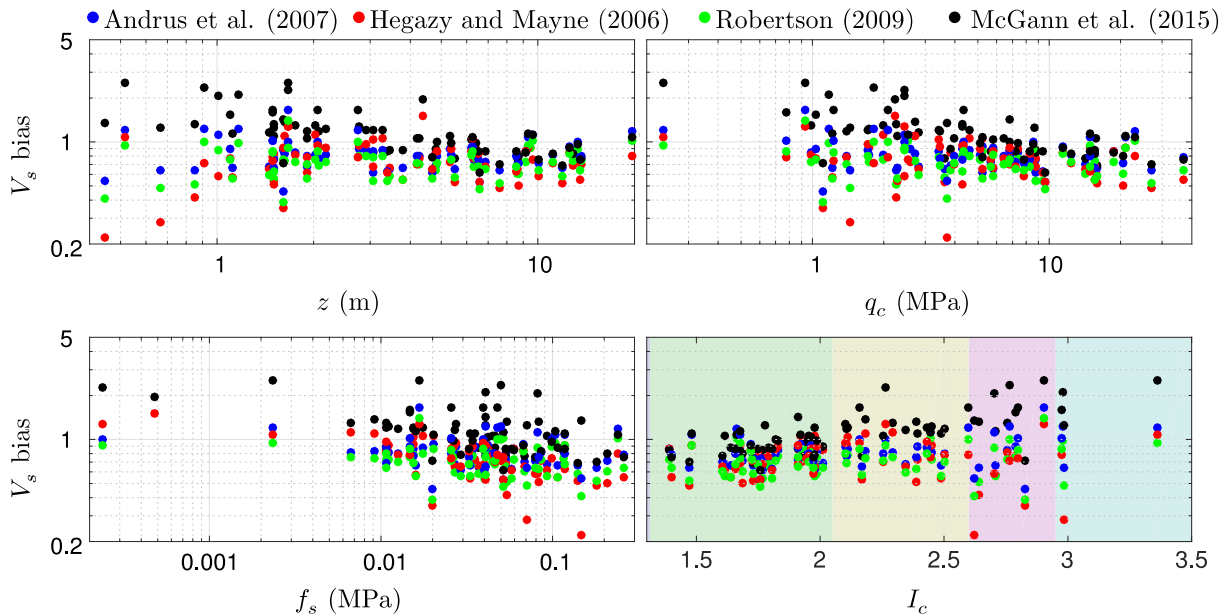

Figure 2. Bias between SW-V$_S$ and CPT-V$_S$ values plotted against z and CPT parameters q$_t$, f$_s$, and I$_c$. Soil behavior type zones indicated by shaded regions in I$_c$ plot are the same as in Figure 1.
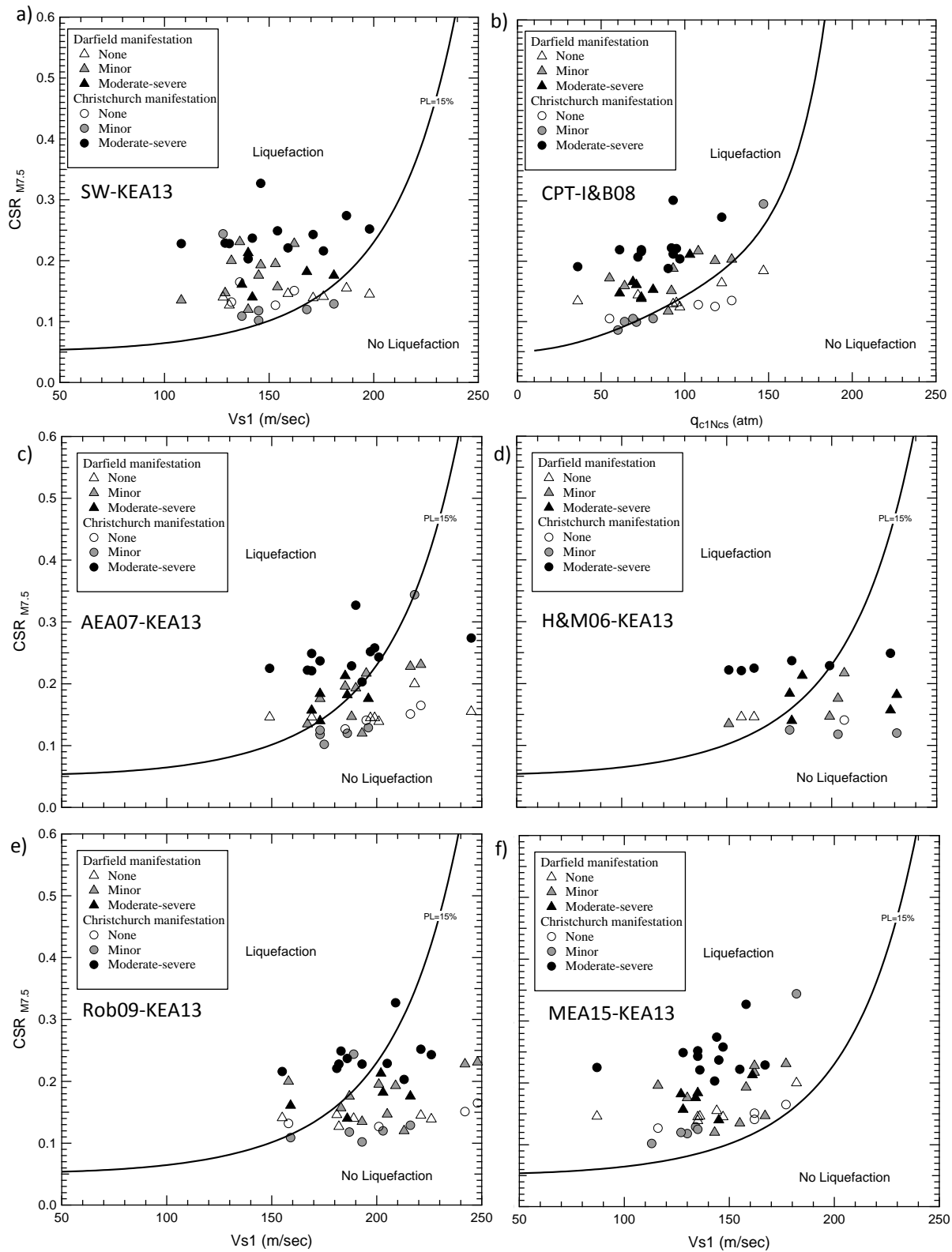
Figure 3. Liquefaction case history data plotted together with CRR$_{M7.5}$ curves: a) Surface wave V$_S$ data analyzed using KEA13, b) CPT q$_{c1Ncs}$ data analyzed using I&B08, c) AEA07 V$_S$ data analyzed using KEA13, d) H&M06 V$_S$ data analyzed using KEA13, e) Rob09 V$_S$ data analyzed using KEA13, f) MEA15 V$_S$ data analyzed using KEA13.

4.2   Liquefaction Triggering Performance

From the liquefaction case histories developed in Green et al. (2014) and Wood et al. (2017), 44 case histories were selected to evaluate the performance of the four CPT-V_S correlations in terms of liquefaction triggering using the KEA13 approach. The KEA13 approach was chosen because it had a lower error index for this dataset than other V_S-based liquefaction triggering relationships (Wood et al., 2017). Although the KEA13 procedure is presented within a probabilistic framework, this comparison focuses only on the deterministic approach, which is associated with a probability of liquefaction of 15%.

For each case history, average values of CSR, cyclic resistance ratio (CRR), and V_{S1} were computed by averaging the parameters across the critical layer to develop single values for comparison. Since both preferred and alternative critical layers are available at some sites, the critical layer choice (either preferred or alternative) that provides the best performance for a particular method was used for the comparison. This provides the most equitable comparison for the data. For more details on the values used for the comparison, refer to Wood et al. (2017).

In Figure 3, the case history data are plotted along with the CRR curves for a magnitude 7.5 earthquake (i.e., $CRR_{M7.5}$) and for 1 atm initial vertical effective confining stress (σ'_{v0}). In Figure 3a, the SW-V_S data is plotted for the KEA13 procedure, while in Figure 3b, the CPT data (i.e., q_{c1Ncs}) for the I&B08 procedure is plotted. These plots provide the baselines for comparisons of the CPT-V_S results shown in Figures 3c-f, where 3c is AEA07, 3d is H&M06, 3e is Rob09, and 3f is MEA15 (each for the KEA13 procedure). To evaluate and compare the predictive performance for each dataset, the error index approach of Green et al. (2014) and Wood et al. (2017) is used. This error index (E_I) is computed as the absolute value of CSR-CRR for each case history that is mispredicted, and is assigned a value of zero for each case history that is correctly predicted. Therefore, if all case histories are correctly predicted the E_I would be zero. However, the E_I will be greater than zero and increase as the "number" and "magnitude" of the mispredictions increase. To insure a neutral comparison, a weight factor of 1.0 is used for all mispredictions, meaning that the misprediction of no liquefaction case histories is weighted the same as the misprediction of positive liquefaction case histories. This ensures that under- and over-estimates of V_S are treated equally in the E_I calculations. This is a departure from the weighted error approach used in Wood et al. (2017), but mirrors that used by Green et al. 2014.

The average E_I for each liquefaction evaluation procedure and V_S profile are provided in Figure 4 and Table 1. Comparing the E_I values, the direct measurement methods (SW and I&B08) clearly provide lower error indices for the case histories analyzed, with the I&B08 approach providing a lower E_I of 0.155 compared to the SW E_I of 0.357. This is an expected outcome, as direct measurement of properties is always preferred over correlated properties. In addition, the better performance of the I&B08 approach is expected due to fact that the critical layers were chosen based upon the CPT measurements

rather than V_S measurements, and indicates that the CPT measurements used in the correlations are of a high quality and provide good performance for liquefaction triggering evaluations.
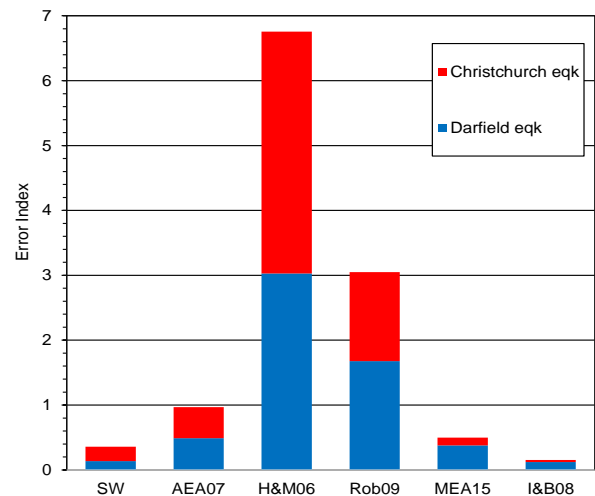
Table 1. Average error indices across all case history sites. Lowest error indices between preferred and alternative critical layer interpretations shown.

Method	Error Index		
	Dar eqk	Chch eqk	Total for all sites
SW	0.136	0.220	0.357
AEA07	0.488	0.480	0.969
H&M06	3.030	3.725	6.755
Rob09	1.676	1.374	3.050
MEA15	0.378	0.119	0.498
I&B08	0.121	0.034	0.155

Figure 4. Average error indices across all case history sites. Lowest error indices between preferred and alternative critical layer interpretations shown.

Comparing the error indices of the four CPT-V_S correlations, the H&M06 and Rob09 correlations have significantly higher E_I values (6.755 and 3.050 respectively) than the AEA09 and MEA15 correlations (0.969 and 0.498, respectively). In Figure 3, comparing the case history positions in relation to the CRR line for the direct measurement results (plots a and b) to the correlated case history results (plots c-f), the AEA07, H&M06, and Rob09 correlated data have a clear shift to the right (i.e., higher V_{S1} values compared to the direct measurements). This shift to the right indicates these correlations tend to predict a higher liquefaction resistance than the direct measurements. In contrast, the MEA15 correlation appears to have a less significant shift to the left, indicating a tendency to predict lower liquefaction resistances than the direct measurement approaches.

To ensure that the reported error indices are not overly influenced by a small number of high error case histories,
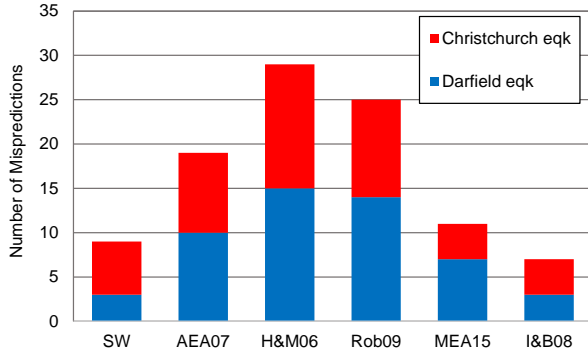
Figure 5. Number of incorrect case history predictions across all case history sites. Values are the lowest between preferred and alternative critical layer interpretations.

the total number of mispredictions for each approach are provided in Figure 5. Similar to the E_I results, the direct measurement methods provide the lowest number of mispredictions. Although the number of mispredictions using each CPT-V_S correlation is still greater than that of SW-V_S, the magnitude of the difference is much less (i.e., the percent difference between the number of mispredictions is far lower than the percent difference in E_I). This indicates the number of mispredictions (especially for the MEA15 correlation) are not significantly different, but the amount of the error (CSR-CRR) is less for the direct measurements than for the CPT-V_S correlations.

To understand the shift in the case history data developed from the CPT-V_S correlations, the difference in V_{S1} within the critical layer between the SW-V_S and each CPT-V_S method is shown in Figure 6 as a function of the average depth of the critical layer. Although the SW-V_S values are used as the baseline for comparisons, it does not imply that the SW-V_S is 100% correct, but given the lower error indices of the SW-V_S results, they provide the best baseline for comparison. Similar to the direct comparisons of the V_S profiles in Figure 1 and 2, the H&M06 and Rob09 correlations systematically over-predict V_{S1} compared to the SW-V_S results, which also matches the observations from the liquefaction triggering plots in Figure 3. The V_{S1} values from the AEA07 correlation also tend to over-predict V_{S1} compared to the SW-V_S results,
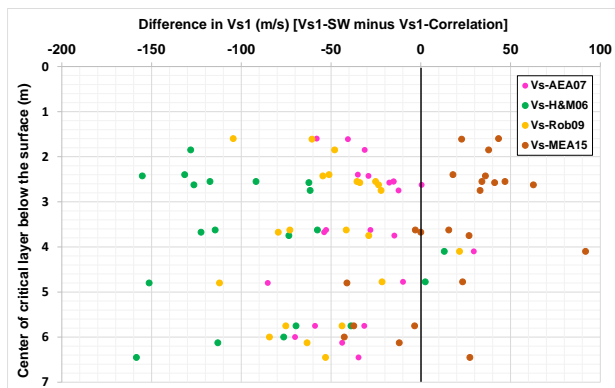

Figure 6. Difference in overburden-corrected shear wave velocity (V_{S1}) within the critical layer between SW-V_{S1} and CPT-V_{S1} as a function of depth to center of critical layer.

Table 2. Average difference in V_{S1} between SW-V_S and CPT-V_S correlations (SW-V_{S1} minus CPT-V_{S1}).

Method	Average difference in V_{S1}			
	Total (+/-) (m/s)	Absolute (m/s)	Total (+/-) (%)	Absolute (%)
AEA07	-32	35	-23	25
H&M06	-120	122	-79	79
Rob09	-51	53	-35	36
MEA15	19	32	11	21

but not as significant. The MEA15 correlation again tends to provide a more balanced estimate, with under-prediction at shallow depths and over-prediction at deeper depths.

To characterize the overall performance, the average differences in V_{S1} between the SW-V_S and CPT-V_S results for all 44 case histories are shown in Table 2. Similar to Figure 3, a clear one-sided over-prediction of V_{S1} values is observed by the AEA07, H&M06, and Rob09 correlations of between 23% and 79%. The MEA15 correlation has an absolute difference of 21%, however, since the correlation tends to both over- and under-predict V_{S1} the total +/- difference is closer to 11%.

5 DISCUSSION AND CONCLUSIONS

Through the analysis of the case history database using all the methods mentioned in the paper, the direct measurement methods (SW-V_S and CPT) preformed the best when predicting liquefaction triggering (i.e., lowest E_I). Three of CPT-V_S correlations (AEA07, H&M06, and Rob09) tend to estimate higher liquefaction resistances than noted from field observations. This behavior from the CPT-V_S correlations is also observed when comparing the SW-V_S values for the entire V_S profiles. The MEA15 correlation seems to have a more balanced estimate of V_S values (some overestimation near the surface and some underestimation at deeper depths) in comparison to the SW-V_S profiles, and the liquefaction triggering results indicate a trend toward estimation of a lower liquefaction resistance than noted from field observations. While the error indices indicate the MEA15 preformed the best (lowest error indices) of the four CPT-V_S correlations, one should not extrapolate these findings to other case histories blindly. The case history database in this study is weighted heavily with positive liquefaction case histories (33 positive case histories, compared to 11 no liquefaction case histories). This would naturally lead to better performance for methods that tend to produce lower liquefaction resistances (i.e., lower V_{S1} values like MEA15) than methods that tend to produce higher liquefaction resistances (i.e., higher V_{S1} values like AEA07, H&M06, and Rob09). Therefore, for this dataset the MEA15 relationship performed the best out of the CPT-V_S correlations tested, which is somewhat expected because the correlation is Christchurch-specific. However, for other datasets with a better balance between liquefaction and no liquefaction case histories, the performance may be closer between the correlations, especially AEA07.

Another factor that may influence the performance of the correlations is the effect of aging on the V_S values. The SW-V_S and MEA15 values inherently include almost no aging because the SW-V_S profiles and SCPT data used in MEA15 were all collected at sites that had been strongly shaken, and liquefied in many cases, by the Darfield and Christchurch earthquakes. The other CPT-V_S correlations are presumably more heavily weighted with data from sites that are effectively 100's or 1000's of years old relative to either deposition or the last significant earthquake. So, while the MEA15 correlation produced the closest V_S predictions to the SW-V_S results and had the lowest liquefaction triggering error indices for the CPT-V_S correlations the results from this study may not hold for datasets containing more aged soils and/or more no-liquefaction cases histories.

6 ACKNOWLEDGEMENTS

7 REFERENCES

Andrus, R., Mohanan, N., Piratheepan, P., Ellis, B., and Holzer, T. 2007. Predicting shear-wave velocity from cone penetration resistance, *Proc. 4th International Conference on Earthquake Geotechnical Engineering*, Thessaloniki, Greece, June 25-28, Paper No. 1454.

Andrus, R.D. and Stokoe II, K.H. 2000. Liquefaction resistance of soils from shear-wave velocity, *Journal of Geotechnical and Geoenvironmental Engineering*, 126(11): 1015-1025.

Bray, J., Cubrinovski, M., Zuppan, J., and Taylor, M. 2014. Liquefaction effects on buildings in the central business district of Christchurch, *Earthquake Spectra*, 30: 85-109

El-Sekelly, W., Abdoun, T., and Dobry, R. 2016. Liquefaction resistance of a silty sand deposit subjected to preshaking followed by extensive liquefaction, *Journal of Geotechnical and Geoenvironmental* Engineering, 142(4): 04015101

Green, R.A., Cubrinovski, M., Cox, B.R., Wood, C.M., Wotherspoon, L., Bradley, B. and Maurer, B. 2014. Select liquefaction case histories from the 2010–2011 Canterbury Earthquake Sequence, *Earthquake Spectra*, 30(1): 131-153.

Green, R.A. and Olson, S.M. 2015. Interpretation of Liquefaction Field Case Histories for Use in Developing Liquefaction Triggering Curves, *Proc. 6th Intern. Conf. on Earthquake Geotechnical Engineering* (6ICEGE), Christchurch, New Zealand, 2-4 November.

Hegazy, Y. and Mayne, P. 2006. A global statistical correlation between shear wave velocity and cone penetration data. *Proc. GeoShanghai, Site and Material Characterization (ASCE GSP 149)*, 243-248.

Idriss, I.M. and Boulanger, R.W. 2008. *Soil liquefaction During Earthquakes*, Monograph MNO-12, Earthquake Engineering Research Institute, Oakland, CA, 261 pp.

Joh, S.H. 1996. *Advances in Interpretation and Analysis Techniques for Spectral-Analysis-of-Surface-Waves (SASW) Measurements*, Ph.D. Dissertation, Dept. of Civil, Architectural, and Environmental Engineering, University of Texas, Austin, TX, 240 p.

Kayen, R., Moss, R., Thompson, E., Seed, R., Cetin, K., Kiureghian, A., Tanaka, Y., and Tokimatsu, K. 2013. Shear-wave velocity-based probabilistic and deterministic assessment of seismic soil liquefaction potential, *Journal of Geotechnical and Geoenvironmental Engineering*, 139(3): 407-419.

McGann, C.R., Bradley, B.A., Taylor, M.L., Wotherspoon, L.M., and Cubrinovski, M. 2015a. Applicability of existing empirical shear wave velocity correlations to seismic cone penetration test data in Christchurch New Zealand, *Soil Dynamics and Earthquake Engineering*, 75: 76-86.

McGann, C.R., Bradley, B.A., Taylor, M.L., Wotherspoon, L.M., and Cubrinovski, M. 2015b. Development of an empirical correlation for predicting shear wave velocity of Christchurch soils from cone penetration test data, *Soil Dynamics and Earthquake Engineering*, 75: 66-75.

McGann, C.R., Bradley, B.A., Wotherspoon, L.M., and Cox, B.R. 2015c. Comparison of a Christchurch-specific CPT-V_S correlation and V_S derived from surface wave analysis for strong motion station velocity characterisation, *Bulletin of the New Zealand Society for Earthquake Engineering*, 48: 81-91.

Moss, R.E.S., Seed, R.B., Kayen, R.E., Stewart, J.P., Der Kiureghian, A., and Cetin, K.O. 2006. CPT-based probabilistic and deterministic assessment of in situ seismic soil liquefaction potential, *Journal of Geotechnical and Geoenvironmental Engineering*, 132(8): 1032–1051.

Quigley, M.C., Bastin, S., Bradley, B.A., (2013). "Recurrent liquefaction in Christchurch, New Zealand, during the Canterbury earthquake sequence", *Geology*, 41: 419-422. 10.1130/g33944.1

Robertson, P.K. and Wride, C.E. 1998. Evaluation of cyclic liquefaction potential using the cone penetration test, *Canadian Geotechnical Journal*, 35(3): 442-459.

Robertson, P.K. 2009. Interpretation of cone penetration tests – a unified approach, *Canadian Geotechnical Journal*, 46(11): 1337-1355.

Wood, C.M., Cox, B.R., Green, R.A., Wotherspoon, L.M., Bradley, B.A., and Cubrinovski, M. 2017. V_S-based evaluation of select liquefaction case histories from the 2010-2011 Canterbury Earthquake Sequence, *Journal of Geotechnical and Geoenvironmental Engineering*, (in (review).